Structural and Functional Roles of Carotenoids in Chlorosomes

Jakub Pšenčík,[a] Juan B. Arellano,[b] Aaron M. Collins,[c*] Pasi Laurinmäki,[d] Mika Torkkeli,[e] Benita Löflund,[d] Ritva E. Serimaa,[e] Robert E. Blankenship,[c] Roman Tuma,[f] Sarah J. Butcher[d]

Department of Chemical Physics and Optics, Faculty of Mathematics and Physics, Charles University, Prague, Czech Republic[a]; Instituto de Recursos Naturales y Agrobiología de Salamanca (IRNASA-CSIC), Salamanca, Spain[b]; Departments of Biology and Chemistry, Washington University in St. Louis, St. Louis, Missouri, USA[c]; Institute of Biotechnology, University of Helsinki, Helsinki, Finland[d]; Department of Physical Sciences, University of Helsinki, Helsinki, Finland[e]; The Astbury Centre for Structural Molecular Biology, University of Leeds, Leeds, United Kingdom[f]

Chlorosomes are large light-harvesting complexes found in three phyla of anoxygenic photosynthetic bacteria. Chlorosomes are primarily composed of self-assembling pigment aggregates. In addition to the main pigment, bacteriochlorophyll *c*, *d*, or *e*, chlorosomes also contain variable amounts of carotenoids. Here, we use X-ray scattering and electron cryomicroscopy, complemented with absorption spectroscopy and pigment analysis, to compare the morphologies, structures, and pigment compositions of chlorosomes from *Chloroflexus aurantiacus* grown under two different light conditions and *Chlorobaculum tepidum*. High-purity chlorosomes from *C. aurantiacus* contain about 20% more carotenoid per bacteriochlorophyll *c* molecule when grown under low light than when grown under high light. This accentuates the light-harvesting function of carotenoids, in addition to their photoprotective role. The low-light chlorosomes are thicker due to the overall greater content of pigments and contain domains of lamellar aggregates. Experiments where carotenoids were selectively extracted from intact chlorosomes using hexane proved that they are located in the interlamellar space, as observed previously for species belonging to the phylum *Chlorobi*. A fraction of the carotenoids are localized in the baseplate, where they are bound differently and cannot be removed by hexane. In *C. tepidum*, carotenoids cannot be extracted by hexane even from the chlorosome interior. The chemical structure of the pigments in *C. tepidum* may lead to π-π interactions between carotenoids and bacteriochlorophylls, preventing carotenoid extraction. The results provide information about the nature of interactions between bacteriochlorophylls and carotenoids in the protein-free environment of the chlorosome interior.

Photosynthetic bacteria comprise a large and diverse group of microorganisms that colonize a variety of ecological niches, including low-light biomes in deep aquatic environments. Some of these low-light niches are inhabited by green photosynthetic bacteria, which have adapted to their environmental conditions by harboring large light-harvesting complexes, the chlorosomes (1–3). A typical chlorosome is an ellipsoidal body (approximately 150 by 50 by 20 nm) with a lipid-protein envelope (4) and an internal core that contains a large number (50,000 to 250,000) of bacteriochlorophyll (BChl) molecules (5, 6). Chlorosomes are located on the cytoplasmic side of the plasma membrane and interface with the membrane via a so-called baseplate. The baseplate is composed of a regular array of the chlorosomal protein CsmA, forming a complex with BChl *a* and carotenoid molecules. BChl *a* serves as an acceptor of the harvested excitation energy from the main chlorosome pigments (BChl *c*, *d*, or *e*). In species belonging to the phyla *Chlorobi* and *Acidobacteria*, the baseplate is further connected to an acceptor protein, FMO (7), while chlorosomes from species belonging to the *Chloroflexi* are directly connected to the membrane. In both cases, the excitation energy is ultimately delivered to the reaction centers within the membrane, where charge separation takes place, and is subsequently used to drive cellular processes.

The internal architecture of chlorosomes is substantially different from that of other photosynthetic antennas, which contain pigments tightly associated with a protein structural scaffold. Instead, the majority of pigments in chlorosomes are arranged in large, self-assembling aggregates with no involvement of proteins. In all structurally characterized chlorosomes, the aggregates consist of chlorin rings stacked into curved sheets that further assemble into lamellae (3, 7–10). The lamellar spacing is proportional to the average length of esterifying alcohols of BChls (11). In the most ordered chlorosomes from *Chlorobaculum tepidum* (especially from a *bchQRU* triple mutant), these lamellae have been described in the form of multilayered cylinders (12, 13).

In addition to BChls, the chlorosome interior also harbors various amounts of carotenoids, which provide photoprotection and also contribute to light harvesting (14–17). *In vitro* assembly studies in aqueous buffers have also suggested that hydrophobic carotenoids may augment self-assembly of BChls into aggregates by enhancing interaction between the hydrophobic tails of esterifying alcohols within lamellae (18, 19). Furthermore, carotenoids can be extracted from chlorosomes isolated from several species by nonpolar solvents, such as hexane (9, 20). Structural characterization of hexane-treated chlorosomes from *Chlorobium phaeovibrioides* (containing BChl *e* as the main pigment) demonstrated that carotenoids are located within lamellae and increase the apparent spacing between adjacent lamellar layers (9).

Among the structurally characterized chlorosomes, those from brown *Chlorobi* species (*C. phaeovibrioides* and *Chlorobium phaeo-*

bacteroides) and the *Chloroflexi* species *Chloroflexus aurantiacus* may accumulate large amounts of carotenoids (up to a carotenoid-to-BChl molar ratio of ~0.5:1) (21, 22). In comparison with *C. tepidum*, all of these species contain a greater percentage of BChl homologs with longer esterifying alcohols, and thus, their aggregates exhibit larger lamellar spacing that allows the accumulation of additional carotenoids (10). In addition, chlorosomes with larger spacing have a more disordered lamellar system, which is manifested, e.g., by a wider distribution of the lamellar spacings seen in electron cryomicroscopy (cryo-EM) and X-ray scattering (9).

Here, we probe the structural role of carotenoids in BChl *c*-containing chlorosomes from two different phyla: *C. aurantiacus* (*Chloroflexi*) and *C. tepidum* (*Chlorobi*). By subjecting purified *C. aurantiacus* chlorosomes to hexane extraction, followed by structural characterization by cryo-EM and X-ray scattering, we demonstrate that carotenoids are, as in the *Chlorobi*, located within lamellae, contributing to the large spacing. Remarkably, the overall structure, including the proteinaceous paracrystalline baseplate, remains intact throughout hexane extraction. In contrast, the carotenoid content in *C. tepidum* chlorosomes is much lower and could not be further reduced with hexane following the same extraction procedure. This difference is ascribed to stronger carotenoid-BChl interactions in *C. tepidum* chlorosomes caused by the specific molecular structure of its pigments.

MATERIALS AND METHODS

Cell growth. *C. tepidum* cells were cultured and chlorosomes were isolated as previously described (8). *C. aurantiacus* cells were grown in a 14-liter fermentor (~30-cm vessel diameter) at two different light intensities: the low-light culture was grown under illumination by four 25-W incandescent bulbs. The fermentor was shielded by a sheet of white paper to diffuse the incident light, resulting in a light intensity of ~10 to 15 μE · m^{-2} · s^{-1} incident to the vessel surface. The culture was grown for 11 days under these conditions to the late exponential phase of growth. The high-light culture was grown under the illumination of 12 100-W incandescent bulbs, leading to a flux of ~1,000 μE · m^{-2} · s^{-1} incident to the vessel surface. The high-light culture was grown for 2 days under these conditions. Both cultures were grown at 50°C in a modified version of DG medium (24) with the following changes: 2 g per liter yeast extract, 1 g per liter Tris base, 0.2 g per liter (NH$_4$)$_2$SO$_4$ adjusted to pH 8.2. In both instances, the cultures did not reach the stationary phase of growth.

C. aurantiacus chlorosomes were isolated using a modified method of Feick and Fuller (25). Whole cells were disrupted using a Branson sonifier, and the suspension was centrifuged at 16,000 × *g* for 20 min. The supernatant was centrifuged at 225,000 × *g* for 2 h at 4°C. The pellet containing whole membranes was resuspended in 20 mM Tris, pH 8, and homogenized using an overhead stirrer with a Teflon mixer. Concentrated whole membranes were diluted to a final optical density at 865 nm (OD$_{865}$) of 2 to 4 cm^{-1} in 2 M NaI and 20 mM Tris, pH 8. The mixture was briefly sonicated and then ultracentrifuged for 16 h at 135,000 × *g* at 4°C. This yielded a floating pellet enriched in chlorosomes, while the supernatant contained mostly membranes. The floating pellets were pooled and resuspended in 20 mM Tris, pH 8. These partially purified chlorosomes were layered onto a two-step (20 to 40% [wt/vol]) sucrose gradient in 20 mM Tris, pH 8, and centrifuged at 135,000 × *g* for 16 h at 4°C. Purified chlorosomes banded at the interface of the gradient layers and pure chlorosomes were collected from the top of the band, while membranes still contaminated the lower part of the band. To further reduce the possibility of membrane and wax oleosome contamination, the top band was subjected to a second sucrose gradient after dilution with 1 volume of 20 mM Tris, pH 8. The final chlorosome stock was suspended in ~20% (wt/vol) sucrose, 20 mM Tris, pH 8.0. After each step of the purification, an absorption spectrum was collected from the various fractions. Comparison of the chlorosomes contaminated with membranes and the final pure chlorosomes showed similar absorption band structures (results not shown), suggesting the chlorosomes used in the subsequent analysis are representative. The selective removal of carotenoids from chlorosomes by a hexane wash was performed as described previously (9).

Pigment analysis. An aliquot of chlorosomes with an OD of 4 cm^{-1} at 742 nm was dried in a centrifugal evaporator at room temperature in the dark. Pigments from the dried chlorosomes were extracted in 500 μl ice-cold 1:1 (vol/vol) acetone-methanol (MeOH). Extracts were bath sonicated for 5 min, followed by incubation of the mixture at −20°C for 20 min. Samples were then centrifuged at 14,000 × *g* for 5 min, and the supernatants were immediately analyzed by high-performance liquid chromatography (HPLC) using a Zorbax Eclipse XDB-C$_{18}$ column (5-μm particle size; 4.6 by 250 mm). The mobile phase was as follows: 0 to 10 min, isocratic flow of 100% methanol; 10 to 18 min, a linear gradient from 100% methanol to 75% methanol and 25% hexane; 18 to 25 min, an isocratic flow of 75% MeOH and 25% hexane. The flow rate was 2 ml · min^{-1}.

Structural analysis. Electron cryomicrographs of chlorosomes from *C. tepidum* were obtained as previously described (8). Cryo-EM data with chlorosomes from *C. aurantiacus* were collected using a Gatan 626 cryoholder maintained at −180°C in a FEI Tecnai F20 microscope operated at 200 kV and recorded with a Gatan Ultrascan 4000 digital charge-coupled device (CCD) camera with a 15-μm pixel size. The magnifications were ×50,000 (*C. tepidum*) and ×109,000 (*C. aurantiacus*). Medium-angle X-ray-scattering data were collected as previously described (8, 11). Samples for X-ray-scattering experiments were concentrated using an ultracentrifuge and airfuge to an OD (at 750 nm) of >500 cm^{-1}.

RESULTS

Absorption spectra. Figure 1a shows absorption spectra of the chlorosomes from *C. aurantiacus* grown under low-light and high-light conditions. The Q$_y$ band of the BChl *c* aggregates is located around ~740 nm and that of BChl *a* around 795 nm. Low-light chlorosomes exhibit greater absorbance in the carotenoid region (~400 to 550 nm), mainly due to higher carotenoid content (relative to BChl *c*) (Table 1) and partly also due to stronger scattering of the low-light chlorosomes caused by their larger size (see below). Figure 1b shows the absorption spectrum of chlorosomes from *C. tepidum*. The differences between the absorption spectra of the two species are mainly due to the small molar fraction of carotenoids and BChl *a* relative to BChl *c* in *C. tepidum* (Table 1).
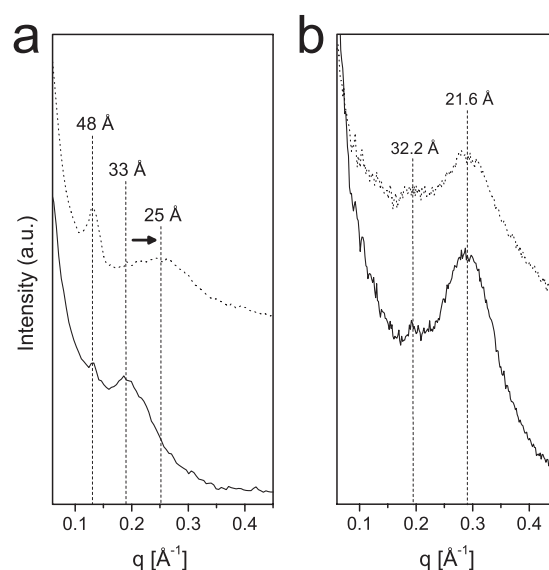
A hexane wash (9, 20) was applied to low-light chlorosomes of *C. aurantiacus* because their carotenoid-to-BChl *c* molar ratio was higher, and therefore, a more pronounced effect was expected. Figure 1a illustrates that hexane efficiently extracted carotenoids from chlorosomes of *C. aurantiacus*. However, the absorption spectra also indicated that a small fraction of carotenoids remained resistant to extraction, suggesting these carotenoids might be tightly bound. In addition, a slight broadening of the BChl *c* Q$_y$ band was observed (Fig. 1a), which slowly diminished with time (not shown). In contrast, the absorption spectrum of *C. tepidum* chlorosomes (Fig. 1b) showed hardly any change upon hexane treatment. Carotenoids were not removed, and broadening of the BChl *c* Q$_y$ band was not observed.

X-ray scattering. X-ray scattering is a useful technique to probe structure on the nanometer scale and has been employed to probe the chlorosome interior (8, 11, 26). In our previous study, it proved difficult to obtain chlorosomes of *C. aurantiacus* devoid of membrane contamination, as attested by X-ray-scattering results
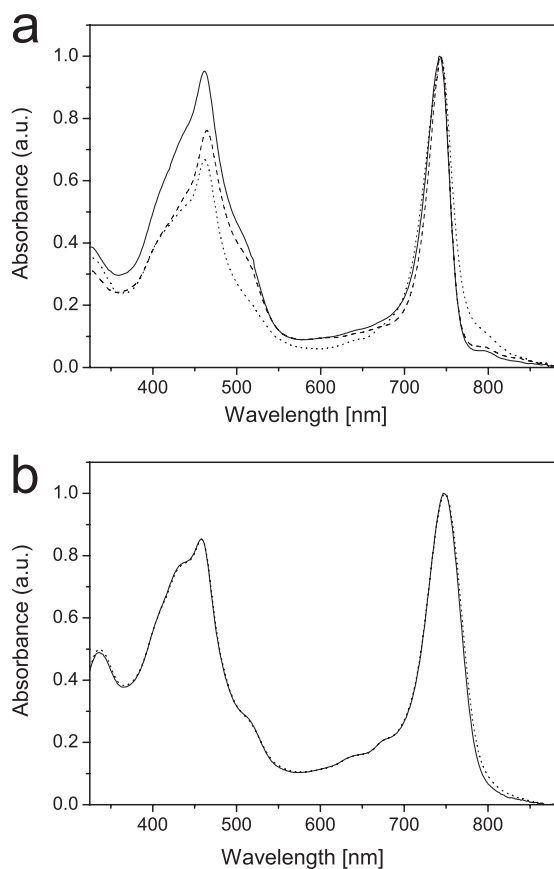
FIG 1 (a) Absorption spectra of chlorosomes from *C. aurantiacus.* Shown are low-light chlorosomes before (solid line) and after (dotted line) the hexane wash and high-light chlorosomes (dashed line). a.u., arbitrary units. (b) Absorption spectra of chlorosomes from *C. tepidum* before (solid line) and after (dotted line) the hexane wash.

FIG 2 X-ray scattering from chlorosomes of *C. aurantiacus* (a) and *C. tepidum* (b) before (solid lines) and after (dotted lines) the hexane wash.

(10). Improved preparation methods yielded chlorosomes with considerably higher purity and consequently resulted in a better X-ray-scattering pattern, although the presence of a peak at a *q* of ~0.13 Å^{-1} suggests some residual contamination with cytoplasmic membranes (Fig. 2a). In particular, the new scattering curve of low-light chlorosomes exhibits a well-resolved lamellar peak at a *q* of ~0.19 Å^{-1} (lamellar spacing, 33 Å) ($q = 4\pi \sin(\theta/2)/\lambda$, where θ is the scattering angle and λ is the X-ray wavelength). A very similar curve was obtained for high-light-grown chlorosomes (data not shown). However, upon extraction of carotenoids by hexane wash, lamellar spacing decreased from 33 to 25 Å (Fig. 2a). In addition, the lamellar peak became slightly broader, perhaps

reflecting the same disorder that caused the broadening of the Q_y absorption band. The decrease of lamellar spacing was confirmed by direct observation using cryo-EM (see below). The membrane peak at ~0.13 Å^{-1} became stronger, presumably due to further stacking of contaminating membranes during hexane treatment induced by their polar surfaces. In contrast, the hexane wash failed to produce any changes in *C. tepidum* X-ray peaks, and thus, the spacing remained the same (Fig. 2b). In addition, the X-ray-scattering pattern demonstrated that the baseplate remained intact in *C. tepidum* after the hexane wash, as demonstrated by the peak corresponding to spacing of 32.2 Å (26). The results show that hexane treatment itself affects neither the lamellar arrangement nor the baseplate integrity, and therefore, the changes in lamellar spacing observed here for *C. aurantiacus*, and previously for *C. phaeovibrioides* (9), are solely due to the carotenoid removal from intact chlorosomes.

Previously, we have reported that the lamellar spacing is proportional to the length of the esterifying alcohol and is further increased by carotenoids within the chlorosome interior (11). For the high-light and low-light chlorosomes of *C. aurantiacus* used in this study, the weighted average of the content of C_{16} and C_{18} esterifying alcohols was determined by HPLC and found to be similar. The resulting average lengths for the esterifying alcohols were as follows: *C* = 17.1 for high-light chlorosomes and *C* = 17.4

TABLE 1 Pigment compositions of the chlorosomes used in this work

	Molar ratio		Esterifying alcohols of BChl *c*	
Bacterium and conditions	BChl *c*/BChl *a*	Carotenoid/BChl *c*	C_{12}:C_{16}:C_{18}[a]	Avg length[b]
C. aurantiacus, high light	27.5:1	0.26:1	0.00:0.34:0.65	17.14
C. aurantiacus, low light	34.5:1	0.31:1	0.00:0.31:0.69	17.38
C. aurantiacus, low light, hexane washed	34.0:1	0.06–0.07:1	0.00:0.32:0.68	17.36
C. tepidum[c]	110:1	0.08:1	0.83:0.17:0.00	12.68

[a] Molar ratio between BChl *c* homologs esterified with alcohols containing different numbers of carbons in the main chain of the alcohol.

[b] Average length of esterifying alcohols expressed as the number of carbons in the main chain of the alcohol.

[c] Data from reference 9.
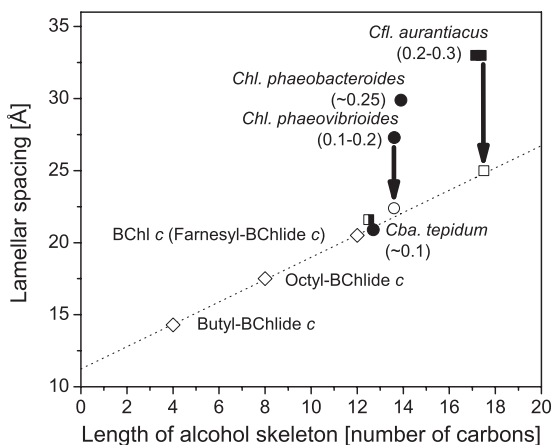
FIG 3 Lamellar spacing of BChl aggregates as a function of the esterifying alcohol length and hexane removal of carotenoids. Data compiled for reference from our previous studies are as follows: diamonds, *in vitro* aggregates ([11](#)); solid circles, native chlorosomes ([8, 9](#)); and open circle, *C. phaeovibrioides* chlorosomes after hexane wash ([9](#)), which is indicated by an arrow. The data obtained in this work are shown as squares. For *C. aurantiacus*, two filled squares are shown for the high-light and low-light chlorosomes and one empty square for low-light chlorosomes after hexane wash. The half-filled, half-empty square for *C. tepidum* reflects the fact that the same spacing was observed before and after the hexane wash. For *C. tepidum*, another point is shown (solid circle) to illustrate the natural batch-to-batch variation in spacing. The numbers in parentheses are carotenoid-to-BChl molar ratios determined for native chlorosomes.

for low-light chlorosomes ([Table 1](#)), where *C* stands for the number of carbons in the main chain of the esterifying alcohol tail. They also accumulated relatively high but comparable fractions of carotenoids ([Table 1](#)) and hence exhibited similar lamellar spacing ([Fig. 3](#)). However, after the extraction of carotenoids, the lamellar spacing decreased, while the average length of the alcohol remained unaffected.

Cryo-EM. To analyze the effect of the hexane wash on overall morphology, the chlorosomes were imaged by cryo-EM. The field views presented in [Fig. 4](#) show that both *C. tepidum* and *C. aurantiacus* chlorosomes remained intact and neither the overall morphology nor the chlorosome internal arrangement was altered by hexane washing, in accordance with previous observations for the BChl *e*-containing green sulfur bacterium *C. phaeovibrioides* ([9](#)).

[Figure 5](#) analyzes the details of representative individual *C. aurantiacus* chlorosomes. High-light chlorosomes were relatively thin and exhibited striations from the baseplate lattice perpendicular to the long axis of the chlorosome and BChl *c* lamellae more or less parallel to the long axis of the chlorosome. On the other hand, low-light chlorosomes were more electron dense, presumably due to a higher content of pigments, leading to thicker chlorosomes. The molar ratios of BChl *c* to BChl *a* and of carotenoids to BChl *c* increased by approximately 25% and 20%, respectively, compared with the high-light chlorosomes ([Table 1](#)). This is further supported by the absorption spectra ([Fig. 1](#)). Consequently, the baseplate is not directly visible in the cryo-EM projections. In addition, low-light chlorosomes exhibited domains of well-ordered lamellar aggregates with variable orientations with respect to the long axes of the chlorosomes ([Fig. 5c](#)). The analysis of Fourier transform power spectra for both types of chlorosomes yielded spacings ranging typically from 26 to 38 Å. The baseplate spacing was about 33 Å, as previously reported ([10](#)).

Cryo-EM further confirmed the decrease of the lamellar spacing after the hexane wash. Fourier transform power spectra yielded values for the spacing typically between 23 and 24 Å. In addition, the micrographs indicated that the internal arrangement of chlorosomes from *C. aurantiacus* remained intact after the hexane wash, including the baseplate and lamellar arrangement in domains ([Fig. 5c](#)). It is worth noting that the systematic difference between the spacings derived from X-rays and cryo-EM is most likely due to underrepresentation of large spacings in EM data analysis. Areas with visible striations, which were selected for the EM analysis, usually correspond to better-ordered and thus tightly packed regions with smaller spacings ([9](#)).

DISCUSSION

The chlorosomes from *C. aurantiacus* studied in this work contained a larger amount of pigments (see below) and had an ~20% higher carotenoid-to-BChl *c* molar ratio when the cells were grown under low-light conditions than when grown under high light. Although the observed increase of the carotenoid fraction was not great, its impact on absorption between ~400 and 500 nm was quite significant ([Fig. 1](#)). The observed higher carotenoid-to-BChl *c* molar ratio under low-light conditions may seem contradictory compared with earlier results obtained for *C. aurantiacus*. Previously, a higher content of carotenoids was observed in extracts from whole cells grown under high-light conditions ([27](#)) and also in chlorosomes isolated from such cells ([22](#)). However, the majority of the additional carotenoids were most probably not located in chlorosomes but within structures known as wax oleosomes ([28](#)), which may copurify with chlorosomes but which were effectively eliminated from our preparation (see Materials and Methods). These additional carotenoids most likely provide photoprotection to cells as screening pigments, but not directly to the BChls associated with chlorosomes, as suggested previously ([10, 11](#)). Based on the present results, we suggest that the amount of carotenoids per BChl *c* molecule inside chlorosomes from *C. aurantiacus* increases moderately under low-light conditions to enhance light harvesting. However, it is not clear whether the observed changes in pigment composition were caused solely by the differences in illumination intensity or if other factors, like cell density or culturing time, also affected the molar ratio of pigments. Therefore, more experiments are needed to further clarify this issue, preferably using continuous cultures and/or identical culturing times.

The combination of X-ray scattering and cryo-EM allowed us to discern features of both the baseplate and the BChl aggregates. Although X-ray scattering from the baseplate overlaps with that from BChl *c* lamellae in chlorosomes for *C. aurantiacus*, cryo-EM projections clearly show the baseplate lattice. Conversely, the X-ray peak from the baseplate is visible for chlorosomes from *C. tepidum*, whereas the baseplate is not discernible in cryo-EM projections because of the thickness of chlorosomes that contain a large amount of BChl *c* relative to BChl *a* ([Table 1](#)). Thus, the observation of the baseplate, either in X-ray (*C. tepidum*) or in cryo-EM (*C. aurantiacus*), for the hexane-washed chlorosomes suggests that the baseplate remains intact during the treatment. Additionally, as attested by cryo-EM, the overall morphology is unaffected by hexane treatment. Thus, the removal of carotenoids and the concomitant change in lamellar spacing happens without changing the chlorosome intactness. On the other hand, a slight broadening of the BChl *c* Q_y band and the lamellar X-ray peak
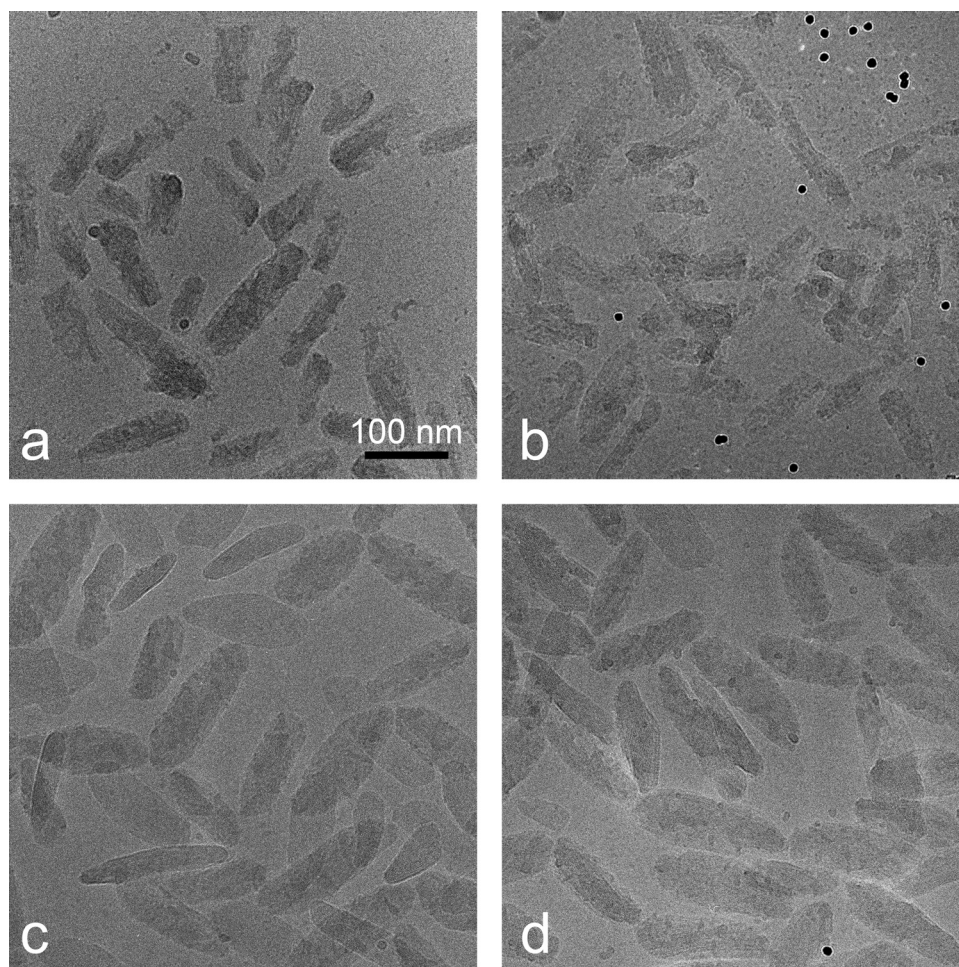
FIG 4 Comparison of overall shapes from electron micrographs of chlorosomes from *C. aurantiacus* grown under low-light conditions (a and b) and *C. tepidum* (c and d) embedded in vitreous ice before (a and c) and after (b and d) hexane wash. The dense 10-nm spheres are from colloidal-gold markers.

were observed in chlorosomes from *C. aurantiacus*, suggesting some disordering of the aggregates accompanying the shrinking of the lamellar spacing during the carotenoid extraction. Nevertheless, the unchanged position of the Q_y band excludes any significant changes in short-range interactions. These spectral changes are similar to those observed for *C. phaeovibrioides* (9).

While the increase of the carotenoid-to-BChl ratio needs to be confirmed by further experiments, the other observed differences between the low-light and high-light chlorosomes are in line with other available data. Previously, it was observed that the overall amount of pigments increases with decrease of the light intensity, in chlorosomes from both *Chlorobi* species (light intensities above $1\ \mu E \cdot m^{-2} \cdot s^{-1}$) (21, 23) and *C. aurantiacus* (22). In this work, we observed changes in morphology between the high-light and low-light chlorosomes that are in a very good agreement with these observations. The high-light chlorosomes from *C. aurantiacus* are relatively thin, and therefore, the baseplate is discernible. In contrast, the low-light samples contain proportionally more BChl *c* and carotenoids than BChl *a* (Table 1). This is in agreement with previously reported pigment ratios under different light conditions (22). As a result, low-light chlorosomes are thicker and the baseplate is not visible in top views. A plausible explanation may be that the high-light chlorosomes correspond to the stage of mor-

phogenesis in which the baseplate is already formed and only a few layers of BChl aggregates are assembled. While this stage is final under high-light conditions, further BChl layers assemble on top of the initial layers under low-light conditions. Indeed, thickening of chlorosomes that correlated with an increase in the ratio of BChl *c* to BChl *a* was observed during chlorosome morphogenesis in *C. aurantiacus* (29). The additional layers in low-light chlorosomes are often arranged into domains of lamellar aggregates with slightly different orientations with regard to the long axis of the chlorosome, although with much less variation than in *C. phaeovibrioides* (9). This might indicate that formation of domains is a general response to low-light conditions and may assist in light harvesting (9).

The mechanism of the domain formation is not yet clear. For certain bacteria from phylum *Chlorobi*, it has been observed that they respond to low-light conditions by producing BChl homologs with longer esterifying alcohols (30, 31). One explanation could be that the newly synthesized homologs do not fit into the spacing of the existing lamellar system and start to nucleate independently of the parallel lamellar system underneath, leading to domain formation. At the same time, more carotenoids are incorporated into the chlorosome. As there is no significant difference between the average lengths of the esterifying alcohols for the low-
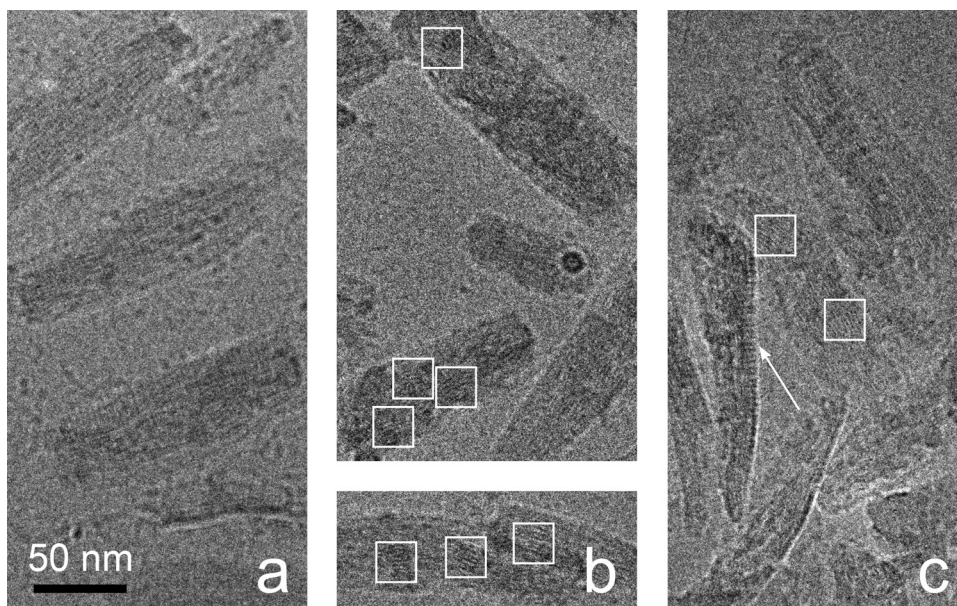
FIG 5 Electron micrographs of representative high-light (a), low-light (b), and hexane-washed low-light (c) chlorosomes from *C. aurantiacus* embedded in vitreous ice. The boxes denote regions where the domains are most pronounced. The arrow indicates a chlorosome where the baseplate is clearly visible and intact after the hexane wash.

light and high-light chlorosomes in this study (Table 1), we have to consider another possibility: The larger amount of pigments produced under low-light conditions may lead to a higher probability of defects during the build-up of the parallel lamellar system, which in turn leads to independent nucleation and domain formation. A similar finding was reported for *C. phaeobacteroides* chlorosomes; whereas parallel lamellae without domains were observed in thin chlorosomes, domains prevailed in thicker chlorosomes (9).

Carotenoids can be effectively removed from the *C. aurantiacus* chlorosome by hexane (20). Here, we have shown that the extraction leads to a substantial decrease in lamellar spacing. Figure 3 demonstrates that the lamellar spacing in BChl aggregates is linearly proportional to the average length of esterifying alcohols in the absence of carotenoids (11). In chlorosomes, the spacing is often larger than that extrapolated by the linear dependence. This deviation is caused by carotenoids, which occupy the lipophilic space of the interdigitated esterifying alcohols between the layers of stacked chlorin rings. When carotenoids are extracted by hexane, the spacing reduces to a value close to that predicted by the average length of the alcohol chains. Similar results were previously obtained for *C. phaeovibrioides* (Fig. 3) (9), which belongs to the phylum *Chlorobi*. Thus, partitioning of carotenoids into the interlamellar space is a general feature of chlorosomes from both *Chloroflexi* and *Chlorobi*. The spacing change for *C. aurantiacus* is larger than that for *C. phaeovibrioides*, which can be explained by the larger amount of carotenoids in the former.

In contrast to *C. aurantiacus*, the efficiency of carotenoid removal by hexane is severely reduced for *C. tepidum* chlorosomes. Although rather efficient removal of carotenoids and quinones by hexane was reported for *C. tepidum* (32), we could not extract carotenoids from *C. tepidum* chlorosomes under the conditions used here for *C. aurantiacus*. This is intriguing, because both *C. aurantiacus* and *C. tepidum* contain BChl *c* as the main pigment.

We cannot explain this as due to differences between *Chlorobi* and *Chloroflexi* species, because the hexane wash was as efficient for *C. phaeovibrioides* as for *C. aurantiacus* under the same conditions. One of the differences between chlorosomes from these two species and those from *C. tepidum* is that the amount of carotenoids is naturally low in *C. tepidum* ($\sim$0.1:1 relative to BChl *c*). These carotenoids seem to be packed in the voids between C_{12} esterifying alcohols within the lamellae. This is probably the main reason why even before the hexane wash the spacing is close to that predicted by the length of the esterifying alcohol chains (Fig. 3). From the data presented in Fig. 3, it seems very likely that when the molar ratio of carotenoids to BChl *c* is about 0.1:1 or below, the carotenoids are filling only the empty spaces between esterifying alcohols in lamellae without affecting the spacing. This may yield a well-defined and ordered interior structure, but it still does not explain why the carotenoids cannot be efficiently removed from the interior of *C. tepidum* chlorosomes by hexane.

One explanation for the low efficiency of carotenoid extraction could be that most of the carotenoids in chlorosomes from *C. tepidum* may be contained within the baseplate, where they are tightly bound to the CsmA protein. Moreover, in *C. aurantiacus* and *C. phaeovibrioides*, a small portion of carotenoids resisted hexane extraction, suggesting a different environment, such as the baseplate. However, the amount of carotenoids in the baseplate is much smaller than the fraction of tightly bound carotenoids in *C. tepidum*. On the basis of the molar ratios for BChl *a* to BChl *c* and for carotenoids to BChl *c* (Table 1), it is possible to calculate that the molar ratio between carotenoids and BChl *a* is about 9. As it is assumed that there are only 2 to 3 carotenoids per BChl *a* molecule in the baseplate (33), we conclude that a substantial portion of the carotenoids in *C. tepidum* must be located in the chlorosome interior. Thus, the presence of baseplate-associated carotenoids cannot fully explain why we found it impossible to remove all carotenoids from *C. tepidum* chlorosomes. On the other hand, the
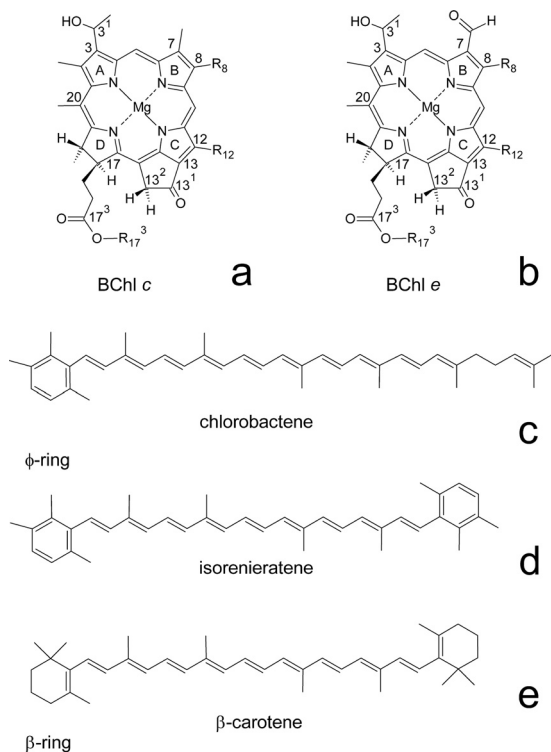
FIG 6 Chemical structures of BChl *c* (a), BChl *e* (b), chlorobactene (c), isorenieratene (d), and β-carotene (e).

FIG 7 Schematic representation of the proposed π-π interaction between the ϕ end of the carotenoids (orange squares with tails) and pyrrole B of the BChl molecules (green squares with tails).

molar ratio between carotenoids remaining in chlorosomes from *C. aurantiacus* after hexane wash and BChl *a* is about 2:1 (Table 1) and matches well the ratio expected for the baseplate pigments. Therefore, we suggest that the carotenoids not extracted by hexane from the *C. aurantiacus* chlorosomes are those located in the baseplate.

We propose the following explanation for the differences in efficiency of carotenoid removal from the chlorosome interiors of different species. We hypothesize that it is based on the molecular details of BChl-carotenoid interactions in chlorosomes. Unlike other light-harvesting complexes, the chlorosome interior is devoid of protein that would control the optimal mutual distances and orientations of the pigments. Thus, pigment-pigment interactions drive assembly, determine the resulting structure and stability, and ensure close contact between the carotenoid and BChl molecules, which in turn is required for the observed efficient excitation energy transfer. Chlorosomes from *Chlorobi* mainly possess carotenoids with one or two aryl rings, namely, ϕ end groups, such as chlorobactene (*C. tepidum*) or isorenieratene (*C. phaeovibrioides*) (Fig. 6). The conjugated system of the ϕ-ring is effectively disconnected from the conjugated system of the carotenoid backbone, and therefore, it does not alter the spectral coverage of the carotenoid absorption in the visible region compared to their precursors (γ-carotene and β-carotene) in their biosynthetic pathway (34). Therefore, there must be a reason other than light harvesting for these bacteria to synthesize carotenoids with the ϕ-ring. It has been suggested that the π-π interaction between the planar conjugated systems of the ϕ-ring and the BChl chlorin is responsible for the close contact between the two molecules (34). Since BChl-BChl π-π stacking plays an important role in

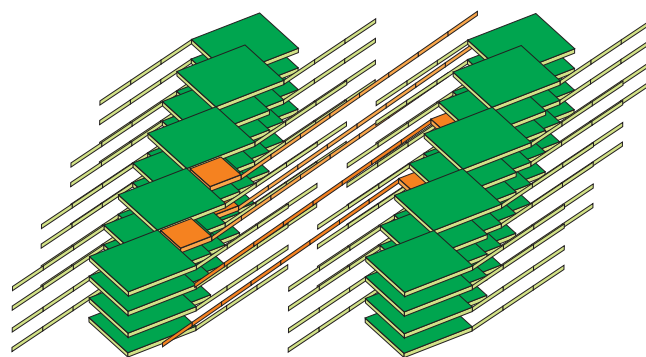stabilization of the aggregate (35), it is likely that the same is true for BChl-carotenoid interactions in chlorosomes from *Chlorobi* species. It is reasonable to expect that π-π interactions are stronger in BChl *c*-containing *C. tepidum* than in BChl *e*-containing brown bacteria, such as *C. phaeovibrioides*, because the aldehyde group at C-7 of BChl *e* (Fig. 6) might prevent close π-π interaction between the conjugated system of BChl molecules and the ϕ end group of carotenoids. This hypothesis is based on the assumption that the π-π interaction is most likely to take place between the ϕ end of the carotenoid and the pyrrole B of the BChl molecule (Fig. 6 shows the labeling of the pyrrole rings). Pyrroles A and C are not accessible due to the hydrogen-bonding network between BChls (Fig. 7), and pyrrole D is reduced (Fig. 6). Therefore, pyrrole B is the only one available for the BChl-carotenoid π-π interactions, and the aldehyde group located at the pyrrole B in BChl *e* may decrease the strength of the attractive interaction through the repulsive interaction caused by its electronegative oxygen. We may also expect that the interaction between BChl and carotenoid molecules is weaker in *C. aurantiacus* than in *C. tepidum* because the carotenoids present in *C. aurantiacus* (mainly β-carotene and γ-carotene) do not contain ϕ end groups but β-rings, with two out-of-plane methyl substituents. In this case, a CH-π interaction seems to be responsible for the attractive interaction between the carotenoid end ring and the conjugated system of the BChl molecule (36). CH-π interaction is weaker than the π-π interaction, and therefore, β-carotene is more easily removed by hexane than chlorobactene.

In conclusion, the results obtained in this work provide important information about BChl-carotenoid interactions in the protein-free environment of the chlorosome interior. The differences in chemical structure between the pyrrole rings B of BChl *c* and *e* and between β and ϕ end groups of carotenoids seem to affect the strength of this interaction, making the interaction between BChl *c* and carotenoids with the ϕ end group the strongest one. Further research on the nature of the BChl-carotenoid interactions is necessary and is now under way.

ACKNOWLEDGMENTS

REFERENCES

1. **Blankenship RE, Matsuura K.** 2003. Antenna complexes from green photosynthetic bacteria, p 195–217. *In* Green BR, Parson WW (ed), Light-harvesting antennas in photosynthesis. Kluwer Academic Publishers, Dordrecht, The Netherlands.

2. **Frigaard NU, Bryant DA.** 2006. Chlorosomes: antenna organelles in photosynthetic green bacteria, p 79–114. *In* Shively JM (ed), Complex intracellular structures in prokaryotes. Microbiology monographs, **vol 2**. Springer, Berlin, Germany.

3. **Oostergetel GT, van Amerongen H, Boekema EJ.** 2010. The chlorosome: a prototype for efficient light harvesting in photosynthesis. Photosynth. Res. **104**:245–255.

4. **Pedersen MO, Linnanto J, Frigaard NU, Nielsen NC, Miller M.** 2010. A model of the protein-pigment baseplate complex in chlorosomes of photosynthetic green bacteria. Photosynth. Res. **104**:233–243.

5. **Montano GA, Bowen BP, LaBelle JT, Woodbury NW, Pizziconi VB, Blankenship RE.** 2003. Characterization of *Chlorobium tepidum* chloromes: a calculation of bacteriochlorophyll *c* per chlorosome and oligomer modeling. Biophys. J. **85**:2560–2565.

6. **Saga Y, Shibata Y, Ltoh S, Tamiaki H.** 2007. Direct counting of submicrometer-sized photosynthetic apparatus dispersed in medium at cryogenic temperature by confocal laser fluorescence microscopy: estimation of the number of bacteriochlorophyll c in single light-harvesting antenna complexes chlorosomes of green photosynthetic bacteria. J. Phys. Chem. B **111**:12605–12609.

7. **Garcia Costas AM, Tsukatani Y, Romberger SP, Oostergetel GT, Boekema EJ, Golbeck JH, Bryant DA.** 2011. Ultrastructural analysis and identification of envelope proteins of "Candidatus Chloracidobacterium thermophilum" chlorosomes. J. Bacteriol. **193**:6701–6711.

8. **Psencik J, Ikonen TP, Laurinmäki P, Merckel MC, Butcher SJ, Serimaa RE, Tuma R.** 2004. Lamellar organization of pigments in chlorosomes, the light harvesting complexes of green photosynthetic bacteria. Biophys. J. **87**:1165–1172.

9. **Psencik J, Arellano JB, Ikonen TP, Borrego CM, Laurinmaki PA, Butcher SJ, Serimaa RE, Tuma R.** 2006. Internal structure of chlorosomes from brown-colored *Chlorobium* species and the role of carotenoids in their assembly. Biophys. J. **91**:1433–1440.

10. **Psencik J, Collins AM, Liljeroos L, Torkkeli M, Laurinmaki P, Ansink HM, Ikonen TP, Serimaa RE, Blankenship RE, Tuma R, Butcher SJ.** 2009. Structure of chlorosomes from the green filamentous bacterium *Chloroflexus aurantiacus*. J. Bacteriol. **191**:6701–6708.

11. **Psencik J, Torkkeli M, Zupcanova A, Vacha F, Serimaa RE, Tuma R.** 2010. The lamellar spacing in self-assembling bacteriochlorophyll aggregates is proportional to the length of the esterifying alcohol. Photosynth. Res. **104**:211–219.

12. **Ganapathy S, Oostergetel GT, Wawrzyniak PK, Reus M, Chew AGM, Buda F, Boekema EJ, Bryant DA, Holzwarth AR, de Groot HJM.** 2009. Alternating syn-anti bacteriochlorophylls form concentric helical nanotubes in chlorosomes. Proc. Natl. Acad. Sci. U. S. A. **106**:8525–8530.

13. **Oostergetel GT, Reus M, Gomez Maqueo Chew A, Bryant DA, Boekema EJ, Holzwarth AR.** 2007. Long-range organization of bacteriochlorophyll in chlorosomes of *Chlorobium tepidum* investigated by cryo-electron microscopy. FEBS Lett. **581**:5435–5439.

14. **Kim H, Li H, Maresca JA, Bryant DA, Savikhin S.** 2007. Triplet exciton formation as a novel photoprotection mechanism in chlorosomes of Chlorobium tepidum. Biophys. J. **93**:192–201.

15. **van Dorssen RJ, Vasmel H, Amesz J.** 1986. Pigment organization and energy transfer in the green photosynthetic bacterium Chloroflexus aurantiacus. II. The chlorosome. Photosynth. Res. **9**:33–45.

16. **Melo TB, Frigaard NU, Matsuura K, Naqvi KR.** 2000. Electronic energy transfer involving carotenoid pigments in chlorosomes of two green bacteria: *Chlorobium tepidum* and *Chloroflexus aurantiacus*. Spectrochim. Acta A Mol. Biol. Spectrosc. **56**:2001–2010.

17. **Psencik J, Ma YZ, Arellano JB, Garcia-Gil J, Holzwarth AR, Gillbro T.** 2002. Excitation energy transfer in chlorosomes of *Chlorobium phaeobacteroides* strain CL1401: the role of carotenoids. Photosynth. Res. **71**:5–18.

18. **Alster J, Polivka T, Arellano JB, Chabera P, Vacha F, Psencik J.** 2010. β-Carotene to bacteriochlorophyll c energy transfer in self-assembled aggregates mimicking chlorosomes. Chem. Phys. **373**:90–97.

19. **Klinger P, Arellano JB, Vacha FE, Hala J, Psencik J.** 2004. Effect of carotenoids and monogalactosyl diglyceride on bacteriochlorophyll *c* aggregates in aqueous buffer: implications for the self-assembly of chlorosomes. Photochem. Photobiol. **80**:572–578.

20. **Brune DC, Nozawa T, Blankenship RE.** 1987. Antenna organization in green photosynthetic bacteria. 1. Oligomeric bacteriochlorophyll c as a model for the 740 nm absorbing bacteriochlorophyll c in Chloroflexus aurantiacus chlorosomes. Biochemistry **26**:8644–8652.

21. **Borrego CM, Garcia-Gil LJ.** 1995. Rearangement of light harvesting bacteriochlorophyll homologues as a response of green sulfur bacteria to low light intensities. Photosynth. Res. **45**:21–30.

22. **Schmidt K, Maarzahl M, Mayer F.** 1980. Development and pigmentation of chlorosomes in *Chloroflexus aurantiacus* strain Ok-70-fl. Arch. Microbiol. **127**:87–97.

23. **Borrego CM, Gerola PD, Miller M, Cox RP.** 1999. Light intensity effects on pigment composition and organisation in the green sulfur bacterium Chlorobium tepidum. Photosynth. Res. **59**:159–166.

24. **Hanada S, Pierson B.** 2006. The family Chloroflexaceae, p 815–842. *In* Dworkin M, Falkow S, Rosenberg E, Schleifer KH, Stackebrandt E (ed), The prokaryotes. Springer, Berlin, Germany.

25. **Feick RG, Fuller RC.** 1984. Topography of the photosynthetic apparatus of *Chloroflexus aurantiacus*. Biochemistry **23**:3693–3700.

26. **Ikonen TP, Li H, Psencik J, Laurinmaki PA, Butcher SJ, Frigaard NU, Serimaa RE, Bryant DA, Tuma R.** 2007. X-ray scattering and electron cryomicroscopy study on the effect of carotenoid biosynthesis to the structure of *Chlorobium tepidum* chlorosomes. Biophys. J. **93**:620–628.

27. **Larsen KL, Cox RP, Miller M.** 1994. Effects of illumination intensity on bacteriochlorophyll c homolog distribution in *Chloroflexus aurantiacus* grown under controlled conditions. Photosynth. Res. **41**:151–156.

28. **Blankenship RE, Olson JM, Miller M.** 1995. Antenna complexes from green photosynthetic bacteria, p 399–435. *In* Blankenship RE, Madigan MT, Bauer CE (ed), Anoxygenic photosynthetic bacteria. Kluwer Academic Publisher, Dordrecht, The Netherlands.

29. **Sprague SG, Staehelin LA, Dibartolomeis MJ, Fuller RC.** 1981. Isolation and development of chlorosomes in the green bacterium *Chloroflexus aurantiacus*. J. Bacteriol. **147**:1021–1031.

30. **Guyoneaud R, Borrego CM, Martinez-Planells A, Buitenhuis ET, Garcia-Gil LJ.** 2001. Light responses in the green sulfur bacterium Prosthecochloris aestuarii: changes in prosthecae length, ultrastructure, and antenna pigment composition. Arch. Microbiol. **176**:278–284.

31. **Mallorqui-Fernandez N.** 2003. Estudi dels carotenoides en especies marrons de bacteris verds del sofre: diversitat, eco-fisiologia i regulacio. Ph.D. thesis. University of Girona, Girona, Spain.

32. **Frigaard NU, Matsuura K, Hirota M, Miller M, Cox RP.** 1998. Studies of the location and function of isoprenoid quinones in chlorosomes from green sulfur bacteria. Photosynth. Res. **58**:81–90.

33. **Montano GA, Wu HM, Lin S, Brune DC, Blankenship RE.** 2003. Isolation and characterization of the B798 light-harvesting baseplate from the chlorosomes of *Chloroflexus aurantiacus*. Biochemistry **42**:10246–10251.

34. **Fuciman M, Chabera P, Zupcanova A, Hribek P, Arellano JB, Vacha F, Psencik J, Polivka T.** 2010. Excited state properties of aryl carotenoids. Phys. Chem. Chem. Phys. **12**:3112–3120.

35. **Alster J, Kabelac M, Tuma R, Psencik J, Burda JV.** 2012. Computational study of short-range interactions in bacteriochlorophyll aggregates. Comput. Theor. Chem. **998**:87–97.

36. **Wang YL, Mao LS, Hu XC.** 2004. Insight into the structural role of carotenoids in the Photosystem I: a quantum chemical analysis. Biophys. J. **86**:3097–3111.